Human Molecular Genetics, 2013, Vol. 22, No. 21 **4339–4348**
doi:10.1093/hmg/ddt283
Advance Access published on June 16, 2013

MCTP2 is a dosage-sensitive gene required for cardiac outflow tract development

Seema R. Lalani[1,†,*], Stephanie M. Ware[4,†], Xueqing Wang[2], Gladys Zapata[1], Qi Tian[1], Luis M. Franco[1], Zhengxin Jiang[1], Kristine Bucasas[1], Daryl A. Scott[1], Philippe M. Campeau[1], Neil Hanchard[1], Luis Umaña[1], Ashley Cast[4], Ankita Patel[1], Sau W. Cheung[1], Kim L. McBride[6], Molly Bray[7], A. Craig Chinault[8], Barbara A. Boggs[8], Miao Huang[9], Mariah R. Baker[3], Susan Hamilton[3], Jeff Towbin[5], John L. Jefferies[5], Susan D. Fernbach[1], Lorraine Potocki[1] and John W. Belmont[1,2]

[1]Department of Molecular and Human Genetics, [2]Children's Nutrition Research Center, Department of Pediatrics and [3]Department of Molecular Physiology and Biophysics, Baylor College of Medicine, Houston, TX, USA [4]Division of Molecular Cardiovascular Biology and [5]The Heart Institute, Cincinnati Children's Hospital Medical Center, Cincinnati, OH, USA [6]Center for Cardiovascular and Pulmonary Research, Nationwide Children's Hospital, and Department of Pediatrics, College of Medicine, Ohio State University, Columbus OH, USA [7]Department of Epidemiology, UAB School of Public Health, Birmingham, AL, USA [8]Research and Development, GeneDx, Gaithersburg, MD, USA [9]Department of Molecular Pathology, M.D. Anderson Cancer Center, Houston, TX, USA

Received March 28, 2013; Revised May 15, 2013; Accepted June 11, 2013

Coarctation of the aorta (CoA) and hypoplastic left heart syndrome (HLHS) have been reported in rare individuals with large terminal deletions of chromosome 15q26. However, no single gene important for left ventricular outflow tract (LVOT) development has been identified in this region. Using array-comparative genomic hybridization, we identified two half-siblings with CoA with a 2.2 Mb deletion on 15q26.2, inherited from their mother, who was mosaic for this deletion. This interval contains an evolutionary conserved, protein-coding gene, *MCTP2* (multiple C2-domains with two transmembrane regions 2). Using gene-specific array screening in 146 individuals with non-syndromic LVOT obstructive defects, another individual with HLHS and CoA was found to have a *de novo* 41 kb intragenic duplication within *MCTP2*, predicted to result in premature truncation, p.F697X. Alteration of *Mctp2* gene expression in *Xenopus laevis* embryos by morpholino knockdown and mRNA overexpression resulted in the failure of proper OT development, confirming the functional importance of this dosage-sensitive gene for cardiogenesis. Our results identify *MCTP2* as a novel genetic cause of CoA and related cardiac malformations.

INTRODUCTION

Obstructive defects of the left ventricular outflow tract (LVOT) form an important spectrum of cardiovascular malformations that include coarctation of the aorta (CoA), aortic valve stenosis (AVS), hypoplastic left heart syndrome (HLHS), complicated mitral valve stenosis with HLHS and CoA (Shone complex), interrupted aortic arch type A and bicuspid aortic valve (BAV). LVOT defects account for ∼14–20% of all medically significant cardiovascular malformations (1). Familial aggregation of these defects is well-recognized (2,3) and diverse genetic mechanisms with extensive locus and allelic heterogeneity are likely. The existence of families with multiple occurrences of the full range of LVOT lesions strongly suggests the existence of common mechanisms underlying the different anatomic forms (4,5). Mutations in *NOTCH1* have been described in a subset of families with calcific AVS and HLHS (6,7); however, the underlying genetic basis of CoA in the majority of patients remains undetermined. In a review of known cytogenetic associations with cardiovascular malformations, we observed that many individuals with large deletions of 15q26 (MIM # 612626) predominantly have LVOT lesions,

*To whom correspondence should be addressed at: Department of Molecular and Human Genetics, Baylor College of Medicine, 1100 Bates St, Houston, TX 77030, USA. Tel: +1 7137988921; Fax: +1 7137987187; Email: seemal@bcm.edu
†These authors contributed equally to the manuscript.

including CoA and HLHS (8–14) (Supplementary Material, Fig. S1). Congenital diaphragmatic hernia (CDH), also observed in 15q terminal deletions (11–13,15), is known to be associated with hemodynamically significant cardiac anomalies (16,17). However, this association of CDH with significant heart defects is not understood. The role of *COUP-TFII* gene, encoding a transcription factor regulated by the retinoid signaling pathway, within this region on 15q26.2 has been established in angiogenesis, lymphatic development and atrial malformations in animal models (18,19). While *COUP-TFII* is implicated in both CDH (20) and cardiac defects in humans (8,21), it is unclear if the disruption of the gene is indeed responsible for the OT lesions in 15q26 segmental aneusomy. In *COUP-TFII* mouse mutants, the sinus venosus and atria fail to develop past the primitive tube stage (18). Based on the animal histological data and the review of the mapped breakpoints from various published reports (Supplementary Material, Fig. S1), we hypothesized that other dosage-sensitive gene(s) within this region may be responsible for left heart developmental defects in humans. Using array-comparative genomic hybridization (CGH) in two half-siblings with CoA with normal dosage of *COUP-TFII*, we identified microdeletion of the centromeric gene, *MCTP2*, and confirmed the functional importance of this gene in the OT formation in *Xenopus*.

RESULTS

Copy-number variations involving *MCTP2* in LVOT obstructive defects

The diagnostic array-CGH analysis in subject 1 with CoA, developmental delay and dysmorphic features (Fig. 1A and B and Supplementary Material, Table S1) identified an interstitial genomic loss of copy number in the 15q26.2 region, confirmed by fluorescence *in situ* hybridization (FISH) analysis (Fig. 1E and F). His maternal half-sister, subject 2 with CoA and facial dysmorphism, was also found to be deleted for this region (Fig. 1C, D and G). Using bacterial artificial chromosome (BAC) clone RP11-4F5, mosaicism for this deletion was identified in the mother by FISH, with 26% of lymphocytes showing normal hybridization signals (Fig. 1H) and 74% of the cells showing a single hybridization signal for this clone (Fig. 1I). Maternal echocardiogram showed no abnormalities of the LVOT. To address whether the identified deletion was a benign copy-number polymorphism, we reviewed the copy-number variation data in 40 200 individuals subjected to the clinical array-CGH at Baylor Medical Genetics Laboratories. No similar size deletions were identified in the clinical database. In addition, no large variants corresponding to the deleted region were identified in the Database of Genomic Variants (http://projects.tcag.ca/variation/), indicating that there were no significant copy-number polymorphisms in this genomic region. To further characterize the deletion in subject 1, we used the Illumina HumanHap300 array and found copy-number loss of 2.2 Mb encompassing an evolutionary conserved gene, *MCTP2* and a hypothetical protein, *LOC145820* (chr15:92,282,797-94,500,921-hg18), within the deleted interval (Fig. 1E).

We then studied 146 individuals with LVOT cardiac malformations for genomic copy-number alterations involving *MCTP2*, *COUP-TFII* and other flanking genes, using a customized high-definition CGH microarray (Agilent Technologies) with oligonucleotide probes in the chr15:89212888-99847710 genomic region (hg18). This cohort (group 2) included 137 patients with isolated LVOT obstructive defects and 9 individuals with syndromic LVOT, with additional features of developmental delay and/or other congenital malformations. While no genomic alterations were observed for *COUP-TFII* in the 146 subjects studied, the array-CGH revealed an intragenic duplication (Fig. 2A) within *MCTP2* in patient 3, with non-syndromic complex cardiac malformation consisting of HLHS, mitral atresia, CoA, BAV and muscular ventricular septal defect. The 41 kb duplication, spanning from intron 10 to intron 17 of the gene, was confirmed by PCR and interphase FISH analysis (Fig. 2B and C) and was not identified in the unaffected parents (Fig. 2A and C). A 670 bp junction fragment was amplified (Fig. 2C) and sequenced. If fully spliced, the predicted mRNA and translation product would yield a protein with premature truncation at p.F697X (Fig. 2D–F). *MCTP2* spans 180 kb of genomic DNA, with 22 coding exons, encoding an 878 residue protein with three C_2 domains and two transmembrane regions (TMRs). The nonsense allele predicted to result from the intragenic duplication causes truncation within the first TMR of the protein.

Knockdown of *Mctp2* in *Xenopus laevis* embryos

The results from these three subjects strongly suggested that *MCTP2* had an important function in cardiac development. Using reverse transcription-polymerase chain reaction (RT-PCR) and RNA harvested from the developing mouse heart at embryonic day 8.5 (E8.5), E9.5, E10.5, E11.5 and E12.5, we determined that *Mctp2* is expressed during critical phases of primary heart tube maturation and morphogenesis (Supplementary Material, Fig. S2A). The expression of *Mctp2* in the atrioventricular (AV) canal was also confirmed by RT–PCR, using endocardial cushion primitive valve tissue isolated from E14.5 embryos (Supplementary Material, Fig. S3). To functionally evaluate the role of *Mctp2* in cardiac development, we carried out loss of function experiments in *X. laevis* embryos. Two morpholino antisense oligonucleotides (MO) were created to target the splice donor of exon 5 (MO1) or splice acceptor of exon 6 (MO2). The *in vivo* efficiency of splice blocking was tested by harvesting RNA from three stage 25 control or *Mctp2* morphant embryos (MO1 or MO2), and demonstrating decreases in transcript levels (Supplementary Material, Fig. S2B).

We hypothesized that *Mctp2* is a dosage-sensitive gene important for cardiac development and performed morpholino dose titration and synergism experiments to demonstrate the specificity of the morpholino effect (Fig. 3A). Viability was assessed at neurula, late tailbud and stage 46 using different concentrations of morpholino and cardiac phenotypes of surviving embryos were assessed. Synergism experiments, in which two morpholinos are injected at amounts that singly would not cause a phenotype but together demonstrate a specific phenotype, indicate the specificity of the morpholino effect (Fig. 3A). A majority of morphant embryos analyzed at stages 44–46 showed grossly normal development but demonstrated variable degrees of edema, suggesting defects of the cardiovascular system (Fig. 3B–D).

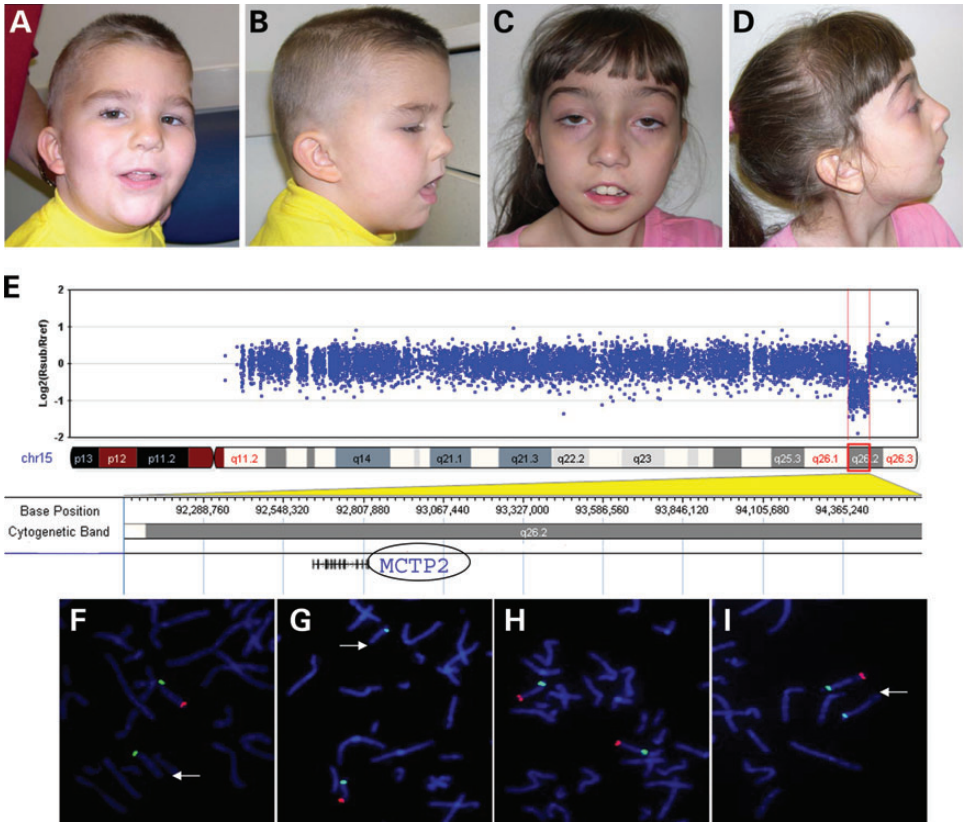

Figure 1. Submicroscopic deletion of *MCTP2* within 15q26.2 in two half-siblings with CoA. (**A** and **B**) Subject 1 and his half-sister, subject 2 (**C and D**) with pertinent features of CoA, microbrachycephaly, malar hypoplasia, thin and down-turned upper lip, posteriorly rotated ears and short stature. (**E**) SNP genotyping using Illumina HumanHap300 BeadChip array showing a 2.2 Mb deletion involving a single gene, *MCTP2* on 15q26.2 in subject 1. (**F**) Genomic loss of copy-number detected by RP11-4F5 in subject 1 showing loss of hybridization signal (red) on one copy of chromosome 15 (shown by arrow). (**G**) These results were also confirmed in his half-sister. Delineation of mosaicism for this deletion in their mother with 26% of her cells showing normal hybridization signals (**H**) and 74% of the cells showing a single hybridization signal for RP11-4F5 (**I**).

Cardiac defects with altered *Mctp2* dosage in *X. laevis*

To further investigate the role of Mctp2 in cardiac development, expression levels of *Mctp2* were altered using single morpholinos, combined morpholinos or *Mctp2* mRNA (Fig. 4). Embryos were scored for cardiac looping and OT position and the development of pericardial edema (Fig. 4A–C). Embryos injected with a sub-effective dose of single *Mctp2* morpholinos did not have increased rates of cardiac defects, but when morpholinos were combined, 70% demonstrated grossly abnormal hearts (Fig. 4A–C). Whole-mount *in situ* hybridization using cardiac troponin was used to better visualize the hearts (Fig. 4B and C).

Embryos were subsequently injected with effective doses of single *Mctp2* morpholinos or *Mctp2* mRNA (Fig. 4D–H) for the evaluation of cardiac histology. Serial transverse sections were collected through the entire cardiac compartment for 53 gain or loss of function *Xenopus* embryos and compared with control embryos and published *Xenopus* cardiac histology (22). MO1-injected embryos were analyzed at stage 44/45 and compared with controls for endocardial cushion formation (Fig. 4D–G). The thin walled atria and a trabeculated ventricle were morphologically distinct. The ventricular myocardium was of normal thickness with well-formed trabeculae in MO1-injected embryos (Fig. 4E), indicating that myocardial differentiation was intact. In control embryos, the endocardial cushion of the developing spiral valve filled the OT throughout its proximal to distal length (Fig. 4D and F). In contrast, sections of *Mctp2* morphant embryos ($n = 17$) showed no evidence of endocardial cushion formation at any level of the developing OT (Fig. 4E and G) in a subset, confirming the critical functional role of *Mctp2* in cardiac OT development. Quantitative analysis showed that 41% of MO1 morphants ($n = 7/17$), 44% of MO2 morphants ($n = 7/16$) and 45% of *Mctp2* mRNA-injected embryos ($n = 9/20$) showed abnormalities of OT development when assessed by histologic analysis of transverse sections (Fig. 4H). Phenotypic defects with both knock down and overexpression of Mctp2 suggest the dosage-sensitive nature of the gene product.

DNA sequencing of *MCTP2* in 146 individuals with LVOT obstructive defects

The *Xenopus* studies indicated that decreases in *Mctp2* may perturb cardiac development, leading us to hypothesize that alterations in MCTP2 protein function in humans might increase susceptibility to congenital heart defects. To investigate this hypothesis, we sequenced the coding exons of *MCTP2* in the same cohort of 146 subjects studied for *MCTP2* dosage. We found heterozygosity for single base changes within *MCTP2* in seven

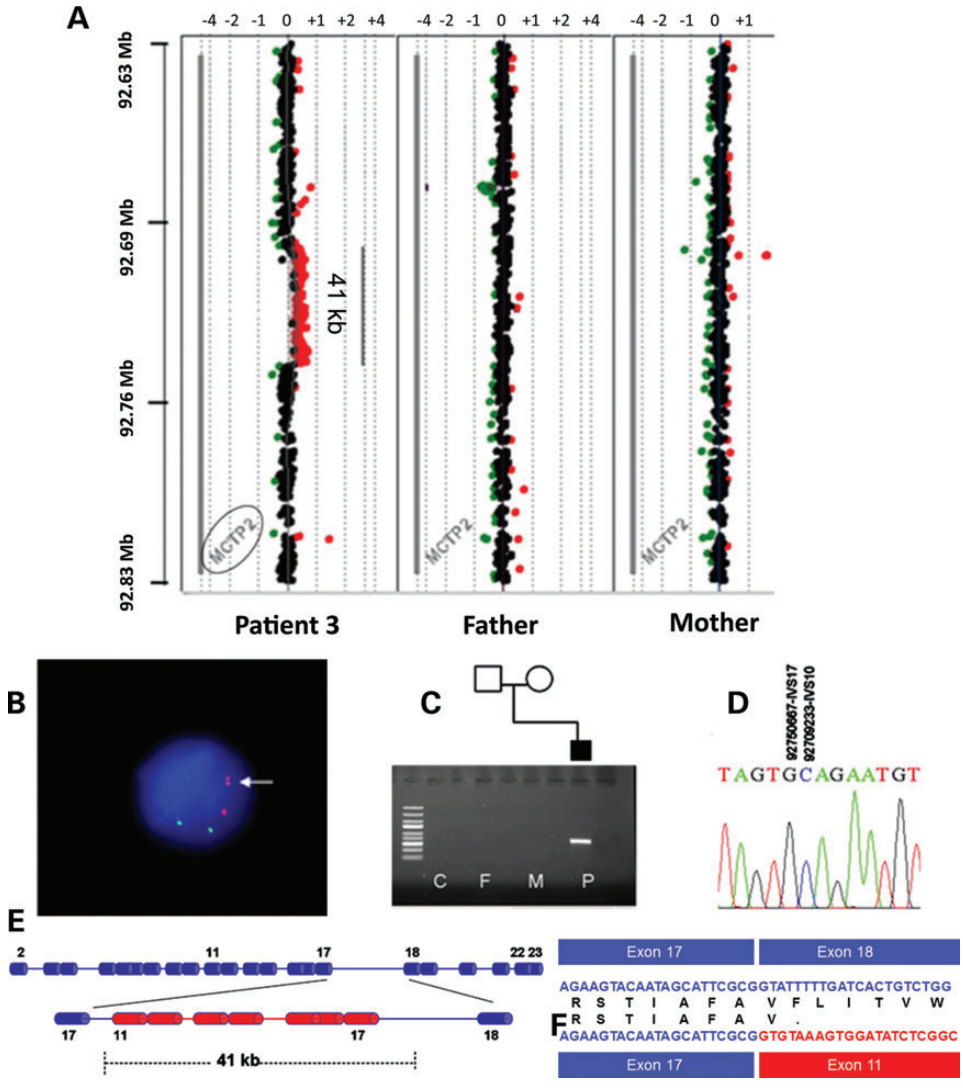

Figure 2. *MCTP2*-specific targeted array-CGH analysis in an individual with HLHS with CoA and breakpoint mapping. (**A**) A 41 kb *de novo* intragenic duplication of *MCTP2* was identified in patient 3 on the targeted array-CGH and was confirmed by interphase fluorescence *in situ* hybridization (FISH) analysis by fosmid (**B**, highlighted by the arrow). (**C**) A junction-specific PCR amplification product was amplified from DNA from patient 3 'P', but not in a control individual 'C', his father 'F' or his mother 'M'. (**D**) DNA sequence from the junction fragment indicating that the breakpoints of the 41 kb duplication lie within intron 17 and intron 10 of the *MCTP2* gene. (**E** and **F**) A schematic representation of the resulting mRNA product with the duplicated fragment is show in red. If correctly spliced, this mRNA is predicted to encode a truncated protein, p.F697X.

subjects with CoA (Supplementary Material, Table S2). In all the cases where parental samples were available, the corresponding variant was identified in one apparently unaffected parent. The variants were also compared against the Exome Variant Server (version ESP6500, accessed at eversusgs.washington.edu), the 1000 Genome Project data (May 2012 update, accessed at.1000genomes.org) and the single nucleotide polymorphism database (build 137, accessed at www.ncbi.nlm.nih.gov). All variants were found in at least one of those databases, albeit at very low minor allele frequencies (Supplementary Material, Table S3). The variants were also assessed in a cohort of 192 apparently unaffected, ethnically matched controls. In this cohort, only variants A60T and G203D were identified, at the heterozygous state in one individual each. A comparison of amino acid sequences in among MCTP2 orthologs showed that glycine203 is highly conserved among the human, rat, mouse, chicken, *Xenopus*, *Caenorhabditis elegans* and zebrafish proteins (Supplementary Material, Fig. S4). The variant G203D, observed in subject 7, with isolated CoA and AVS, was predicted to have deleterious effects by multiple prediction programs, including PolyPhen-2 and SIFT (Supplementary Material, Table S3). This variant was found to be present in his mother. We have previously shown that there is a higher rate of asymptomatic LVOT anomalies including the occurrence of BAV in first-degree relatives of the affected subjects (23); thus, we cannot rule out clinically asymptomatic defects in the parent with this variant. The other variant, Y235C, observed in subject 8 with CoA and mitral stenosis, was found to be paternal in origin and involved amino acid residues that were conserved among human, rat and mouse proteins. Predicted to be damaging

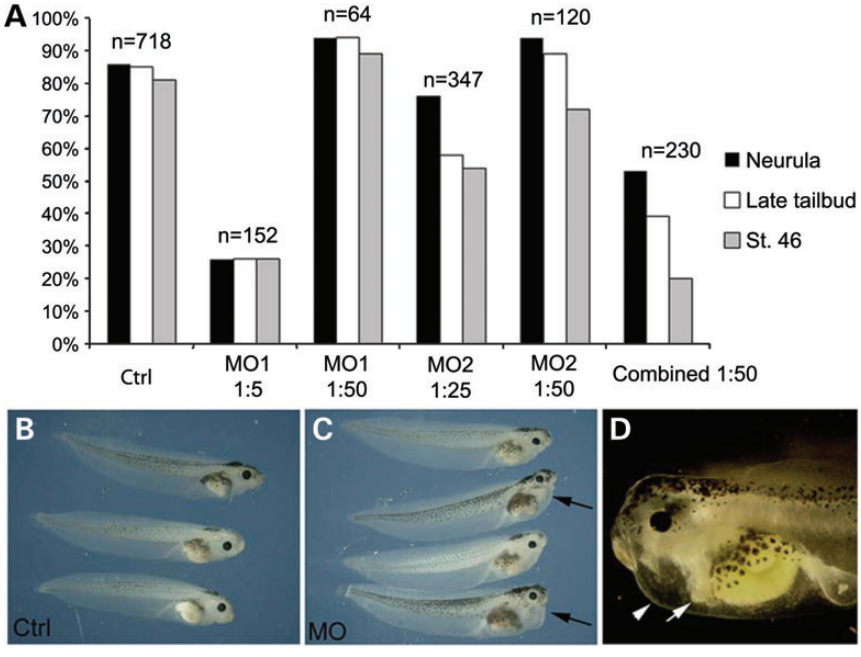

Figure 3. *Mctp2* morphant analyses. (**A**) Embryos were scored for viability at the indicated stages. Sub-effective doses of morpholinos had no effect on phenotype or viability when compared with controls when injected individually [Ctrl, MO1 1:50 (0.54 ng), MO2 1:50 (0.54 ng)]. Morphants injected with both morpholinos at sub-effective doses showed significant decreases in viability. The number of embryos analyzed in each group is represented above each group of bars. (**B**–**D**) Control and *Mctp2* morphant embryo morphology at stage 44/45. Qualitatively similar phenotypic results were achieved using both morpholinos and (C) and (D) are representative images using MO1. (**C**) *Mctp2* morphants have grossly normal external morphology with the exception of moderate to severe edema in a subset of embryos (arrows). (**D**) High power view of embryo with severe edema showing accumulation of fluid (arrowhead) in the cardiac region (arrow at heart).

by PolyPhen-2, this variant was not present in our control cohort or the exome variant server but was found in the 1000 genomes database at a very low frequency (SNP ID rs191271656, minor allele frequency 0.0009). Both variants, G203D and Y235C, were studied further by functional analysis.

Functional analysis of *MCTP2* variants

Since it is known that the C_2A domain of MCTP2 has a high affinity for Ca^{2+} (24), we asked if the two heterozygous base substitutions within the C_2A domain, G203D and Y235C, altered the calcium-binding affinity of the protein. We used terbium (lanthanide metal) fluorescence to compare the Ca^{2+}-binding affinity of expressed wild-type or variant-containing fragments. Terbium directly competes for calcium-binding sites in natural calcium-binding proteins and is intrinsically fluorescent when complexed to protein, with a broad excitation spectrum and an emission maximum at ~545 nm. To assess the differences in relative Ca^{2+}affinity, we used Ca^{2+} (5–50 nM) to decrease the terbium(III) fluorescence at 545 nm (Fig. 5). The competition curves were biphasic for both the wild-type C_2A fragment and G203D and Y235C mutants suggesting two Ca^{2+}-binding sites. The Ca^{2+} IC50 s for wild-type C_2A domain were 524 nM and 27.5 μM; for G203D, 60 nM and 99 μM and for Y235C, 104 nM and 35 μM. Both G203D and Y235C mutants had altered relative affinity for Ca^{2+} with a lower relative affinity at the first Ca^{2+}-binding site (IC50-1, wild-type [wt] versus G203D $P < 0.0001$; wt versus Y235C $P < 0.0001$) and a higher relative affinity at the second Ca^{2+}-binding site, when compared with the wild-type C_2A (IC50-2, wt versus G203D $P < 0.0001$; wt versus Y235C $P = 0.0173$). These results suggest that the G203D and Y235C mutations alter the calcium-binding affinity of the MCTP2 protein.

DISCUSSION

Several individuals have been reported with congenital heart defects in 15q26-ter deletion syndrome (MIM# 612626). Individuals with terminal deletions disrupting *COUP-TFII* often present with septal defects (21,25,26), while OT defects are observed more often when deletions extend centromeric to the gene (8–14). Our findings indicate that disruption of *MCTP2*, which is ~1.9 Mb centromeric to *COUP-TFII*, contributes to congenital left heart obstructive cardiac defects in humans. The following lines of evidence support this conclusion: (i) the 2.2 Mb microdeletion on 15q26.2 involving the *MCTP2* gene with normal dosage of *COUP-TFII* in two individuals with CoA and the absence of this deletion in 40 200 individuals studied by the clinical array-CGH; (ii) a *de novo* intragenic duplication of *MCTP2* predictive of protein truncation in a non-syndromic individual with HLHS and CoA; (iii) functional knockdown of *Mctp2* expression in *Xenopus* resulting in abnormal cardiac development and (iv) identification of rare *MCTP2* missense variants in patients with CoA, which alter the Ca^{2+}-binding affinity of the protein. It is evident from the morpholino experiments that despite its important role in cardiac development, the penetrance for the cardiac phenotype is not complete with *Mctp2* knockdown. This is furthermore apparent from the normal echocardiographic findings of the mother of subjects 1 and 2, who had the *MCTP2* heterozygous deletion in 74% of

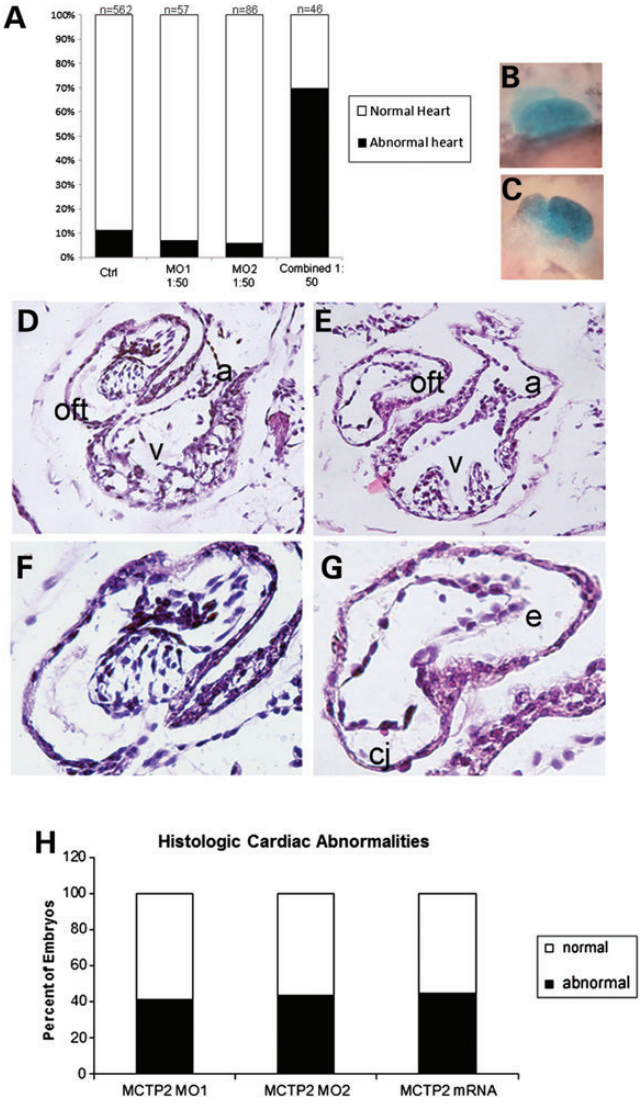

Figure 4. Altering *Mctp2* expression levels causes defects in cardiac development. (**A**) Comparison of rate of cardiac defects in morphants injected at sub-effective morpholino concentrations singly or in combination. (**B** and **C**) Whole-mount *in situ* hybridization with cardiac troponin T illustrates abnormal cardiac morphology in MO1/MO2 morphant (C) when compared with control (B). Representative histological analyses of control (**D** and **F**) and *Mctp2* MO1 (**E** and **G**) embryos at stage 44/45 demonstrate abnormalities of the OT and endocardial cushion formation. (D and E) Posterior/proximal OT at the level of connection with the ventricle. (F and G) High powered views of the developing OT in (D) and (E) are shown. In control embryos, the endocardial cushion of the developing spiral valve fills the OT throughout its proximal to distal length. In contrast, sections of *Mctp2* morphant embryos showed no evidence of endocardial cushion formation at any level of the developing OT, confirming the critical functional role of *Mctp2* in cardiac OT development. (**H**) Percent of embryos with abnormal OT development. Transverse sections were analyzed for *Mctp2* MO1, *Mctp2* MO2 and *Mctp2* mRNA-injected embryos. The number of embryos analyzed for each injection group is indicated above the bar. a, atria; cj, cardiac jelly; e, endocardial cells; ec, endocardial cushion; oft, outflow tract; V, ventricle.

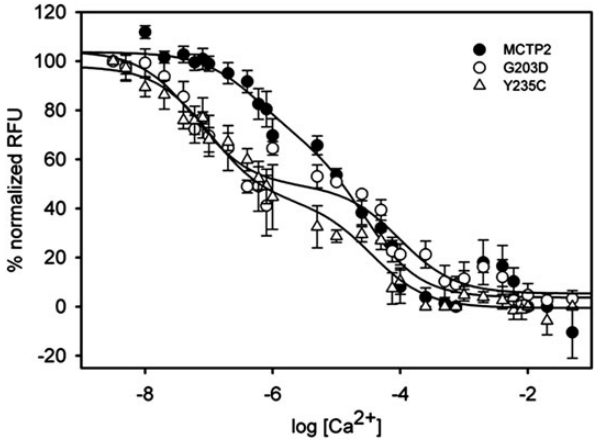

Figure 5. Ca^{2+} titration of the terbium fluorescence showing altered Ca^{2+}-binding affinity of the C_2A domain mutants. Terbium fluorescence was used to monitor the changes in relative affinity of Ca^{2+} for the C_2A domain. Terbium(III) (1 mM) was incubated with MCTP2-C_2A (20 μM) and titrated with Ca^{2+} (5 nM–50 mM). The terbium(III) signal (excitation 285 nm; emission 545 nm) decreased with increasing Ca^{2+} concentrations and the data are plotted as the percent decrease from 0 Ca^{2+}. The IC50 s for the wild-type C_2A are 524 ± 2 nM and 28 ± 1 μM; for G203D are 61 ± 1 nM ($P < 0.0001$ compared with wild-type site 1) and 99 ± 1 μM ($P < 0.0001$ compared with wild-type site 2) and for Y235C are 05 ± 1 nM ($P < 0.0001$ compared with wild-type site 1) and 35 ± 1 μM ($P = 0.0173$ compared with wild-type site 2). Data shown are means ± SEM ($n = 3–6$).

lymphocytes. The observed incomplete penetrance is in keeping with several other genomic disorders that cause cardiovascular malformations (27,28). We note that deletions encompassing *MCTP2* could, in principle, affect regulatory sequences that influence COUP-TFII expression. It is possible that the cardiovascular malformations observed in the subjects described here could be the result of combined effects on *MCTP2* and *COUP-TFII*. However, the data provided here support the hypothesis that *MCTP2* can make a contribution independent of *COUP-TFII*.

MCTPs are composed of a variable N-terminal sequence, three C_2 domains, two TMRs and a short C-terminal sequence (24). Proteins with multiple C_2 domains and a single TMR such as synaptotagmins (29), ferlins (30) and E-Syts (31) are known to be involved in the Ca^{2+}-dependent regulation of exocytosis. The *MCTP2* protein is unusual in that unlike other families of trafficking proteins containing multiple C_2 domains and a single TMR, the C_2 domains of *MCTP2* bind to Ca^{2+} in the absence of phospholipids with a high apparent affinity (24). We show that two rare missense variants in the C_2A domain of *MCTP2* identified in individuals with sporadic CoA alter the calcium-binding affinity of the protein. Future studies focusing on the cell-type-specific role of MCTP2 during cardiac morphogenesis, including its role in Ca^{2+} binding and intracellular trafficking, should provide important insights into novel mechanisms underlying OT development.

The primitive heart tube of the early embryo (E8.0 in mouse) is comprised of an inner layer of endocardial cells and an exterior layer of myocardial cells. As cardiac development proceeds, cells from the second heart field migrate in at the anterior and posterior poles and contribute to the development of the right ventricle, conotruncus and part of the atria. Subsequently, cardiac neural crest cells migrate into the heart following rightward looping (32–34). As development proceeds (at stage 14 in chick and 9.5 ED in mouse embryos), some of the endothelial cells in the OT and AV regions lose their epithelial phenotype, transform into migratory mesenchymal cells and invade the adjacent extracellular matrix, resulting in the formation of

valvuloseptal endocardial cushion tissue (35). The morphogenesis of the endocardial cushion is induced by regionalized myocardial signals in the AV canal and OT regions, causing a subset of endocardial cells to undergo epithelial–mesenchymal transformation (EMT) and invade the cardiac jelly. Endocardial cushions are precursors of the heart valves and contribute to the septation of the atria and ventricles and the remodeling of the OT to form the aorta and the pulmonary artery. In *Mctp2* morphants, the intact myocardial and endocardial layers of the OT in the presence of cardiac jelly suggest failure of the endocardial cells to undergo EMT and highlight an important potential mechanistic basis for the development of structural heart defects that warrants additional investigation. Interestingly, *Notch1*, which is implicated in LVOT abnormalities, such as familial aortic valve anomalies and BAV (6), has been shown to be essential for EMT during endocardial cushion formation (36). *Notch1*-deficient mouse embryos fail to form endocardial cushions and demonstrate an absence of mesenchymal cells migrating from the endocardium. These results are very similar to the phenotypes identified in *Mctp2* morphants. Future studies will determine whether Notch signaling is perturbed with *Mctp2* haploinsufficiency.

Despite the large number of animal models demonstrating defects in cardiac development, single gene causes of human cardiovascular malformations have been more difficult to identify. This study highlights the importance of a novel gene in human cardiovascular malformations. Whether the haploinsufficiency of *MCTP2* causes a broader pleiotropic effect pertaining to neurocognitive and language development, as observed in individuals with 15q26 segmental aneusomies and subjects 1 and 2 in this study remains to be determined as additional cases are identified. Future mechanistic studies of Mctp2 function will provide an opportunity to identify new pathways important for cardiac development. In conclusion, these experiments identify *MCTP2* as a novel dosage-sensitive gene important for human LVOT development and highlight an important role of *MCTP2* in cardiac development.

MATERIALS AND METHODS

Human subjects

Written informed consents were obtained from the research subjects and the study was performed in accordance with the institutional guidelines for human research with approval by the Institutional Review Board at Baylor College of Medicine. Our patients consisted of two groups; group 1 included two maternal half-siblings, subjects 1 and 2 with syndromic CoA and their mother. Group 2 consisted of 146 patients with LVOT obstructive defects, primarily enrolled at Texas Children's Hospital in Houston, TX (included 83 Caucasians, 48 Hispanics, 9 African Americans, 3 Asians and 3 mixed Caucasian/Hispanics). This cohort had 137 patients with isolated cardiac lesions (120 with primary diagnosis of CoA, 10 with HLHS and 7 with Shone complex) and 9 with syndromic LVOT obstructive defects, with additional features of developmental delay and non-cardiac malformations. Each enrolled family was interviewed in person for detailed information on the prenatal course, diagnosis and family history of heart defects. Additional clinical information was obtained through review of the medical records.

Array-CGH, genome-wide SNP genotyping and FISH analyses

Peripheral blood samples from subject 1 in group 1 were submitted for clinical testing to the Baylor Medical Genetics Laboratories for BAC array-CGH analyses. Reciprocal dye reversal experiments were performed as described previously (37). Data analysis was performed by a web-based software platform with the capability of displaying the raw, normalized and integrated data of all clones to detect genomic copy-number changes for patient relative to a gender-matched control. A copy-number loss was determined by a combined $\log_2$ ratio of test/control < -0.2 and a *P*-value of < 0.05. FISH experiments on metaphase cells were performed to confirm the deletion of the region corresponding to BAC clone, RP11-4F5 in subject 1, identified by the clinical array-CGH. Miniprep BAC DNA (100 ng) was labeled with Spectrum Orange-dUTP or Spectrum Green-dUTP (Vysis, Downers Grove, IL, USA), according to the manufacturer's instructions, and used as probes for FISH analysis using the standard protocols (38). To precisely map the deletion breakpoints, genome-wide analysis for DNA copy-number alterations was performed in subject 1 using Illumina HumanHap300 genotyping BeadChip array (317K, Illumina, San Diego, CA, USA) according to the manufacturer's specifications, as described previously (39).

In group 2, 146 patients with LVOT obstructive lesions were studied with a custom high-definition CGH microarray (Agilent Technologies). These arrays included 1004 oligonucleotide probes in the chr15:89212888-99847710 genomic region (hg18), in a 4 × 44k format, spanning exonic, intronic and 5′ and 3′ regions of candidate genes within this interval, including *MCTP2* and *COUP-TFII*. Array data were analyzed using Feature Extraction and CGH Analytics software (Agilent Technologies). The *MCTP2* intragenic duplication of 41 kb was confirmed in patient 3 by PCR and FISH analysis, using fosmid G248P86659A10.

Identification of *X. laevis Mctp2*

Transcript information for *Xenopus tropicalis Mctp2* was derived from the Joint Genome Institute database. Primers were designed in regions highly conserved across species to attempt to amplify *X. laevis* genomic DNA. Primers were designed in the first and second coding exons (177 bp product) and fourth and sixth coding exons (234 bp product; homologous to the fifth and seventh exons in human) for PCR and RT–PCR: exon 1F 5′AGCACTTGGGTTCAAGAGGA 3′; exon 2R 5′ TGAACGTTCCTCAGGCTTTT 3′; exon 4F 5′ CCTTGTACAAAAGCAAGGTCA 3′; exon 6F 5′CCATGTCTTCCTCCAAGCTA 3′. Genomic DNA was isolated from *X. laevis* and used with exon 4 and exon 6 primers for PCR amplification using an annealing temperature of 54°C. The resulting 1038 bp product was PCR purified (Qiagen), sequenced and compared with the *X. tropicalis* database (sequence available upon request). No pseudoalleles were identified within the region sequenced. RNA was prepared from stage 25 *X. laevis* embryos using Trizol as per the manufacturer's protocol. RT–PCR was

performed using Titan One Tube RT–PCR (Roche) with 50 ng template RNA and a post reverse transcription annealing temperature of 54°C. The 234 bp product was purified (Qiagen PCR purification) and sequenced.

Mctps antisense morpholino oligonucleotide and mRNA expression construct

For *X. laevis*, two splice site Mctp2 antisense morpholino oligonucleotides were designed (Gene Tools, LLC). The first MO (MO1) was located at the splice donor site at the junction of exon 5–intron 5; the sequence was 5′ GCG GAA ATA ATT TGA TCA TAC TTG T 3′. The second MO (MO2) was located at the splice receptor site at the junction of intron 5–exon 6 with a sequence 5′ TCT GTA GTT CTA CAT TAG GAA GGA A 3′. Both MOs were fluoroscein tagged. A control antisense morpholino was also obtained from Gene Tools, LLC, with the following sequence 5′ CCT CTT ACC TCA GTT ACA ATT TAT A 3′. All morpholinos were resuspended and stored according to the manufacturer's protocol (Gene Tools, LLC). To verify effective knockdown of the *Mctp2* transcript by each morpholino, three control or morpholino-injected embryos were selected at stage 25 and pooled for homogenization in Trizol. Only grossly normal frog embryos were selected at this stage, and the presence of morpholino was confirmed by the fluorescein expression of the tagged morpholino. The experiment was repeated in triplicate (three separate injection batches with three embryos pooled from MO1, MO2 or control-injected sets; Supplementary Material, Fig. S2B).

For *Mctp2* overexpression studies, full-length human *MCTP2* cDNA was purchased from Open Biosystems (clone 5276211), cloned into pBS and fully sequenced. The construct was linearized with *Bam*HI and transcribed using T7 RNA polymerase using the mMessage mMachine kit as per the manufacturer's instructions to generate full-length capped human MCTP2 mRNA.

Xenopus laevis embryo injections

Xenopus laevis embryos were staged according to Nieuwkoop and Faber (40). Embryos were injected in the animal most part of the blastomere at 1–2 cell stages. Injections were performed in 4% Ficoll and 1/3 Marc's modified ringers (MMR). After injection, embryos were transferred to 0.1× MMR and were allowed to develop at room temperature. *Xenopus* embryos were injected with 5.39 ng MCTP2 MO1 (1:5 concentration) or 1.08 ng MCTP2 MO2 (1:25 concentration). For synergism experiments, each morpholino was used at a dilution of 1:50, such that 0.54 ng MCTP2 MO1 and 0.54 ng MCTP2 MO2 were used.

To confirm efficiency of splice blocking, RT–PCR was performed with primers which span the site of action of the splice blocking MOs. All analyses were performed using stage-matched embryos.

Histology

Embryos were fixed in MEMFA (0.1M MOPS; 2mM EGTA; 1mM MgSO4; 3.7% Formaldehyde) at the appropriate stages, dehydrated in successive ethanol washes, washed twice in xylene and three times in paraffin, and subsequently embedded. Sections were prepared at 8–10 μm using a Leica microtome. Subsequently, slides were dewaxed in xylene, rehydrated through successive ethanol washes and stained with Gill's Haematoxylin and Eosin Y.

Whole-mount *in situ* hybridization

Xenopus embryos were fixed at the desired stage in MEMFA for 2 h at room temperature. Following fixation, embryos were dehydrated in 100% ethanol and stored at −20°C. Whole-mount *in situ* hybridization was performed as described previously (41). The pBSK-Cardiac Troponin plasmid was kindly provided by the Zorn Laboratory and was used to generate antisense riboprobes.

MCTP2 sequencing

Mutation analysis of *MCTP2* was performed in all 146 subjects in group 2, studied for *MCTP2* dosage alteration. The protein-coding exons of *MCTP2* were amplified from genomic DNA (sequence of primers and amplification conditions available on request). The PCR products were purified using ExoSAP-IT (USB Corporation, Cleveland, OH, USA) and sequenced with a dye terminator cycle-sequencing system (Applied Biosystems 3730xl).

Expression and purification of recombinant wild-type and mutant proteins

We performed functional analyses of the two heterozygous base substitutions, G203D and Y235C, within the C_2A domain in two individuals with CoA. The DNA encoding the human *MCTP2*-C_2A (residue 195-286) was PCR amplified, subcloned into pGEX-6p-1 vector (GE Healthcare, NJ, USA) and verified by DNA sequencing. This construct was used for the site-directed mutagenesis. Two missense variants (G203D and Y235C) were constructed using the QuickChange site-directed mutagenesis kit (Stratagene, CA, USA) and verified by DNA sequencing. These plasmids were transformed into *Escherichia coli* strain and expressed as glutathione-S-transferase (GST) fusion proteins, refolded with Rapid GST Inclusion Body Kit (Cell Biolabs, Inc., CA, USA) and purified with Glutathione Sepharose 4 Fast Flow (GE Healthcare). Recombinant GST protein was expressed and purified as control using the same method.

Fluorescence spectroscopy

The relative Ca^{2+}-binding affinity of the three recombinant proteins was assessed by monitoring the changes in terbium(III) fluorescence binding. Buffer (50 mM Tris, pH 7.4, 0.1 M NaCl) was incubated with Chelex resin 100 (Bio-Rad) for 15 min at room temperature to remove trace levels of Ca^{2+}. The Chelex resin was removed by centrifugation before lanthanide metal ion terbium(III) (Sigma) binding. Fluorescence due to terbium(III) (1 mM) binding was recorded on an ISS PCI photon-counting spectrophotometer (Champaign, IL, USA) excited at 285 nm (UV solar pass filter) and the emission spectra (520–570 nm). Ca^{2+} was titrated from 5 to 50 mM. For each recombinant protein, the experiment was repeated three to six times. Emission

maxima (545 nm) at each Ca^{2+} concentration were corrected by subtracting background at 530 nm. These data were normalized, their percent change from 0 Ca^{2+} calculated, and data fit with a two site competition equation using SigmaPlot 10.0.

SUPPLEMENTARY MATERIAL

Supplementary Material is available at *HMG* online.

ACKNOWLEDGEMENTS

We are indebted to the families who participated in the study.

Conflict of Interest statement. None declared.

FUNDING

This work was supported by grants to S.R.L. from the Doris Duke Charitable Foundation and the Gillson Logenbaugh Foundation; the NIH RO1-HL091771 grant to J.W.B. and S.R.L.; Burroughs Wellcome Fund Clinical Scientist Award in Translational Research #1008496 to S.M.W.; and March of Dimes #1-FY10-401 grant to S.M.W. and S.R.L. K.L.M. is supported by K23HL70823.

REFERENCES

1. Hoffman, J.I. and Kaplan, S. (2002) The incidence of congenital heart disease. *J. Am. Coll. Cardiol.*, **39**, 1890–1900.
2. Boughman, J.A., Berg, K.A., Astemborski, J.A., Clark, E.B., McCarter, R.J., Rubin, J.D. and Ferencz, C. (1987) Familial risks of congenital heart defect assessed in a population-based epidemiologic study. *Am. J. Med. Genet. A*, **26**, 839–849.
3. Ferencz, C. and Boughman, J.A. (1993) Congenital heart disease in adolescents and adults. teratology, genetics, and recurrence risks. *Cardiol. Clin.*, **11**, 557–567.
4. Gerboni, S., Sabatino, G., Mingarelli, R. and Dallapiccola, B. (1993) Coarctation of the aorta, interrupted aortic arch, and hypoplastic left heart syndrome in three generations. *J. Med. Genet.*, **30**, 328–329.
5. Wessels, M.W., Berger, R.M., Frohn-Mulder, I.M., Roos-Hesselink, J.W., Hoogeboom, J.J., Mancini, G.S., Bartelings, M.M., Krijger, R., Wladimiroff, J.W., Niermeijer, M.F. *et al.* (2005) Autosomal dominant inheritance of left ventricular outflow tract obstruction. *Am. J. Med. Genet. A*, **134**, 171–179.
6. Garg, V., Muth, A.N., Ransom, J.F., Schluterman, M.K., Barnes, R., King, I.N., Grossfeld, P.D. and Srivastava, D. (2005) Mutations in NOTCH1 cause aortic valve disease. *Nature*, **437**, 270–274.
7. McBride, K.L., Riley, M.F., Zender, G.A., Fitzgerald-Butt, S.M., Towbin, J.A., Belmont, J.W. and Cole, S.E. (2008) NOTCH1 mutations in individuals with left ventricular outflow tract malformations reduce ligand-induced signaling. *Hum. Mol. Genet.*, **17**, 2886–2893.
8. Baptista, J., Mercer, C., Prigmore, E., Gribble, S.M., Carter, N.P., Maloney, V., Thomas, N.S., Jacobs, P.A. and Crolla, J.A. (2008) Breakpoint mapping and array CGH in translocations: comparison of a phenotypically normal and an abnormal cohort. *Am. J. Hum. Genet.*, **82**, 927–936.
9. Choi, J.H., Kang, M., Kim, G.H., Hong, M., Jin, H.Y., Lee, B.H., Park, J.Y., Lee, S.M., Seo, E.J. and Yoo, H.W. (2011) Clinical and functional characteristics of a novel heterozygous mutation of the IGF1R gene and IGF1R haploinsufficiency due to terminal 15q26.2->qter deletion in patients with intrauterine growth retardation and postnatal catch-up growth failure. *J. Clin. Endocrinol. Metab.*, **96**, E130–E134.
10. Davidsson, J., Collin, A., Bjorkhem, G. and Soller, M. (2008) Array based characterization of a terminal deletion involving chromosome subband 15q26.2: an emerging syndrome associated with growth retardation, cardiac defects and developmental delay. *BMC Med. Genet.*, **9**, 2.
11. Klaassens, M., Galjaard, R.J., Scott, D.A., Bruggenwirth, H.T., van Opstal, D., Fox, M.V., Higgins, R.R., Cohen-Overbeek, T.E., Schoonderwaldt, E.M., Lee, B. *et al.* (2007) Prenatal detection and outcome of congenital diaphragmatic hernia (CDH) associated with deletion of chromosome 15q26: two patients and review of the literature. *Am. J. Med. Genet. A*, **143A**, 2204–2212.
12. Scott, D.A., Klaassens, M., Holder, A.M., Lally, K.P., Fernandes, C.J., Galjaard, R.J., Tibboel, D., de Klein, A. and Lee, B. (2007) Genome-wide oligonucleotide-based array comparative genome hybridization analysis of non-isolated congenital diaphragmatic hernia. *Hum. Mol. Genet.*, **16**, 424–430.
13. Slavotinek, A.M., Moshrefi, A., Davis, R., Leeth, E., Schaeffer, G.B., Burchard, G.E., Shaw, G.M., James, B., Ptacek, L. and Pennacchio, L.A. (2006) Array comparative genomic hybridization in patients with congenital diaphragmatic hernia: mapping of four CDH-critical regions and sequencing of candidate genes at 15q26.1–15q26.2. *Eur. J. Hum. Genet.*, **14**, 999–1008.
14. Tumer, Z., Harboe, T.L., Blennow, E., Kalscheuer, V.M., Tommerup, N. and Brondum-Nielsen, K. (2004) Molecular cytogenetic characterization of ring chromosome 15 in three unrelated patients. *Am. J. Med. Genet. A*, **130A**, 340–344.
15. Mosca, A.L., Pinson, L., Andrieux, J., Copin, H., Bigi, N., Puechberty, J., Sarda, P., Receveur, A., Sevestre, H., Pigeonnat, S. *et al.* (2011) Refining the critical region for congenital diaphragmatic hernia on chromosome 15q26 from the study of four fetuses. *Prenat. Diagn.*, **31**, 912–914.
16. Bielinska, M., Jay, P.Y., Erlich, J.M., Mannisto, S., Urban, Z., Heikinheimo, M. and Wilson, D.B. (2007) Molecular genetics of congenital diaphragmatic defects. *Ann. Med.*, **39**, 261–274.
17. Graziano, J.N. (2005) Cardiac anomalies in patients with congenital diaphragmatic hernia and their prognosis: a report from the congenital diaphragmatic hernia study group. *J. Pediatr. Surg.*, **40**, 1045–1049.
18. Pereira, F.A., Qiu, Y., Zhou, G., Tsai, M.J. and Tsai, S.Y. (1999) The orphan nuclear receptor COUP-TFII is required for angiogenesis and heart development. *Genes Dev.*, **13**, 1037–1049.
19. Aranguren, X.L., Beerens, M., Vandevelde, W., Dewerchin, M., Carmeliet, P. and Luttun, A. (2011) Transcription factor COUP-TFII is indispensable for venous and lymphatic development in zebrafish and *Xenopus laevis*. *Biochem. Biophys. Res. Commun.*, **410**, 121–126.
20. You, L.R., Takamoto, N., Yu, C.T., Tanaka, T., Kodama, T., Demayo, F.J., Tsai, S.Y. and Tsai, M.J. (2005) Mouse lacking COUP-TFII as an animal model of Bochdalek-type congenital diaphragmatic hernia. *Proc. Natl Acad. Sci. USA*, **102**, 16351–16356.
21. Nakamura, E., Makita, Y., Okamoto, T., Nagaya, K., Hayashi, T., Sugimoto, M., Manabe, H., Taketazu, G., Kajino, H. and Fujieda, K. (2011) 5.78 Mb terminal deletion of chromosome 15q in a girl, evaluation of NR2F2 as candidate gene for congenital heart defects. *Eur. J. Med. Genet.*, **54**, 354–356.
22. Mohun, T.J., Leong, L.M., Weninger, W.J. and Sparrow, D.B. (2000) The morphology of heart development in *Xenopus laevis*. *Dev. Biol.*, **218**, 74–88.
23. McBride, K.L., Pignatelli, R., Lewin, M., Ho, T., Fernbach, S., Menesses, A., Lam, W., Leal, S.M., Kaplan, N., Schliekelman, P. *et al.* (2005) Inheritance analysis of congenital left ventricular outflow tract obstruction malformations: segregation, multiplex relative risk, and heritability. *Am. J. Med. Genet. A*, **134A**, 180–186.
24. Shin, O.H., Han, W., Wang, Y. and Sudhof, T.C. (2005) Evolutionarily conserved multiple C2 domain proteins with two transmembrane regions (MCTPs) and unusual Ca2+ binding properties. *J. Biol. Chem.*, **280**, 1641–1651.
25. Dateki, S., Fukami, M., Tanaka, Y., Sasaki, G., Moriuchi, H. and Ogata, T. (2011) Identification of chromosome 15q26 terminal deletion with telomere sequences and its bearing on genotype-phenotype analysis. *Endocr. J.*, **58**, 155–159.
26. Poot, M., Eleveld, M.J., van 't Slot, R., van Genderen, M.M., Verrijn Stuart, A.A., Hochstenbach, R. and Beemer, F.A. (2007) Proportional growth failure and oculocutaneous albinism in a girl with a 6.87 Mb deletion of region 15q26.2->qter. *Eur. J. Med. Genet.*, **50**, 432–440.
27. Fontaine, J.L., Vernant, P., Graveleau, D., Lagardere, B. and Elchardus, J.F. (1976) Elfin facies, mental retardation and cardiovascular anomalies (Williams and Beuren's syndrome). Report of two cases. *Ann. Pediatr. (Paris)*, **23**, 37–42.
28. Thienpont, B., Zhang, L., Postma, A.V., Breckpot, J., Tranchevent, L.C., Van Loo, P., Mollgard, K., Tommerup, N., Bache, I., Tumer, Z. *et al.* (2010) Haploinsufficiency of TAB2 causes congenital heart defects in humans. *Am. J. Hum. Genet.*, **86**, 839–849.
29. Sudhof, T.C. (2002) Synaptotagmins: why so many? *J. Biol. Chem.*, **277**, 7629–7632.

30. Bansal, D. and Campbell, K.P. (2004) Dysferlin and the plasma membrane repair in muscular dystrophy. *Trends Cell Biol.*, **14**, 206–213.
31. Min, S.W., Chang, W.P. and Sudhof, T.C. (2007) E-Syts, a family of membranous Ca2+-sensor proteins with multiple C2 domains. *Proc. Natl Acad. Sci. USA*, **104**, 3823–3828.
32. Buckingham, M., Meilhac, S. and Zaffran, S. (2005) Building the mammalian heart from two sources of myocardial cells. *Nat. Rev. Genet.*, **6**, 826–835.
33. Moorman, A.F. and Christoffels, V.M. (2003) Cardiac chamber formation: development, genes, and evolution. *Physiol. Rev.*, **83**, 1223–1267.
34. Srivastava, D. (2006) Making or breaking the heart: from lineage determination to morphogenesis. *Cell*, **126**, 1037–1048.
35. Markwald, R.R., Fitzharris, T.P. and Smith, W.N. (1975) Structural analysis of endocardial cytodifferentiation. *Dev. Biol.*, **42**, 160–180.
36. Timmerman, L.A., Grego-Bessa, J., Raya, A., Bertran, E., Perez-Pomares, J.M., Diez, J., Aranda, S., Palomo, S., McCormick, F., Izpisua-Belmonte, J.C. *et al.* (2004) Notch promotes epithelial-mesenchymal transition during cardiac development and oncogenic transformation. *Genes Dev.*, **18**, 99–115.
37. Lu, X., Shaw, C.A., Patel, A., Li, J., Cooper, M.L., Wells, W.R., Sullivan, C.M., Sahoo, T., Yatsenko, S.A., Bacino, C.A. *et al.* (2007) Clinical implementation of chromosomal microarray analysis: summary of 2513 postnatal cases. *PLoS One*, **2**, e327.
38. Trask, B.J. (1991) Fluorescence in situ hybridization: applications in cytogenetics and gene mapping. *Trends Genet.*, **7**, 149–154.
39. Steemers, F.J. and Gunderson, K.L. (2007) Whole genome genotyping technologies on the BeadArray platform. *Biotechnol. J.*, **2**, 41–49.
40. Nieuwkoop, P.D. and Faber, J. (1994) *Normal Table of* Xenopus laevis (*Daudin*). Garland Publishing Inc., New York.
41. Cast, A.E., Gao, C., Amack, J.D. and Ware, S.M. (2012) An essential and highly conserved role for Zic3 in left-right patterning, gastrulation and convergent extension morphogenesis. *Dev. Biol.*, **364**, 22–31.